Phase diagrams for a binary mixture confined in narrow slitlike pores with energetically heterogeneous walls from a lattice mean-field approach

2003 J. Phys.: Condens. Matter 15 3107

(http://iopscience.iop.org/0953-8984/15/19/312)

INSTITUTE OF PHYSICS PUBLISHING JOURNAL OF PHYSICS: CONDENSED MATTER

J. Phys.: Condens. Matter **15** (2003) 3107–3119 PII: S0953-8984(03)56978-8

Phase diagrams for a binary mixture confined in narrow slitlike pores with energetically heterogeneous walls from a lattice mean-field approach

A Martinez[1], A Patrykiejew[2], O Pizio[3] and S Sokołowski[2]

[1] Facultad de Quimica, UNAM, México DF, Mexico
[2] Department for the Modelling of Physico-Chemical Processes, Faculty of Chemistry, Maria-Curie Skłodowska University, 20031 Lublin, Poland
[3] Institute of Chemistry, UNAM, México DF, Coyoacan 04510, Mexico

Received 29 March 2003
Published 6 May 2003
Online at stacks.iop.org/JPhysCM/15/3107

Abstract

We investigate the phase behaviour of binary symmetric lattice fluid, exhibiting partial demixing in slitlike pores with heterogeneous walls. The calculations are carried out assuming a cubic lattice with vacancies and a model for heterogeneity similar to that of Röcken and Tarazona (1996 *J. Chem. Phys.* **105** 2034). We concentrate on the effects of surface heterogeneity on the scenarios for the phase transformations. It is shown that for wide enough pores a stepwise condensation occurs between demixed phases. For narrower pores the λ-line may cross the boundaries of the bridge phase and multiple critical end points appear. In such cases, at low temperatures the bridge phase formation occurs between demixed phases, at intermediate temperature it involves mixed and demixed phases and finally it becomes a transition between two demixed phases again.

1. Introduction

Surface heterogeneity is an important intrinsic property of adsorbing surfaces. Its presence yields qualitative changes in the behaviour of adsorbed phases, in comparison with phases growing on uniform substrates [1]. Several attempts have been undertaken to characterize heterogeneous surfaces at qualitative and quantitative levels with a reasonable efficiency [1, 2]. In the case of real adsorbing surfaces, the effects of chemical and geometrical heterogeneities are strongly interconnected in a nontrivial manner. However, modelling of heterogeneous adsorbents usually involves assumption of only one type of heterogeneity: energetic or geometrical. Recently, it has become possible to produce solid substrates with controlled nonuniformity. In particular, the advance of technology allows us to construct axially nonuniform adsorbents, i.e. in which the adsorption potential varies only along one of the

axes parallel to the surface [3–6]. The interest in such systems stems from the possibility of development of suitable theoretical approaches. In fact, there exists an abundant literature concerning theoretical study of adsorption at single walls, as well as in porous systems, see e.g. [7–14].

A few years ago Röcken and Tarazona [9] investigated capillary condensation in slitlike pores with structured (i.e. energetically heterogeneous) walls in the framework of a lattice model within a mean-field approximation. To mimic chemical inhomogeneity of real adsorbents [3–6] the adsorbing potential was described by a periodic function along one of the axes parallel to the pore wall. They observed a new mechanism of capillary condensation, characterized by a splitting of the usual capillary condensation coexistence envelope into two branches. One of the phases formed during that process was called 'a bridge phase', because resulting dense adsorbate phases filled only a part (along one of the axes parallel to the pore wall) of the pore, building a kind of bridge between two solid pore walls. Further increase of the bulk gas density (or chemical potential) resulted in the filling of the remaining parts of the pore with a dense, condensed adsorbate. Obviously, the latter process was usual capillary condensation. In subsequent works this model has been generalized to the case of lattice-off systems and studied by means of a density functional theory [9–12]. Both lattice and lattice-off approaches yielded quite similar results and led to qualitatively the same topology of the phase diagrams. Later, similar investigations have been also carried out for one-component fluids with associative interactions [11]. All these studies have revealed a rich variety of possible phase transitions. In addition to the formation of bridge phases, layering-type transitions could also be observed. These transitions take place within consecutive layers adjacent to the pore walls and their occurrence and the number depend on the strength of the fluid–solid potential, as well as on the pore size. Wider discussion of the phase transitions in pores with heterogeneous walls can be found in [8–12].

From the fundamental, as well as from the applicational, point of view the investigation of adsorption of fluid mixtures is much more important than of single-component fluids. Structural and thermodynamic behaviour of bulk mixtures is quite complex [15–20]. Particular classes of mixtures manifest an interplay between the liquid–vapour and demixing transitions. Very recently we have undertaken investigation of the phase behaviour of such fluids in slitlike pores with energetically homogeneous walls by using a density functional approach. The application of that methodology to the case of pores with structured walls would result in time consuming computations, which then would prohibit the study of the phase behaviour in detail. Therefore, we have decided to simplify the modelling of mixtures adsorbed in heterogeneous pores and to apply a lattice model, in conjunction with a mean-field approximation. Nevertheless, such simplification should not lead to a loss of the principal physical phenomena we want to study.

The aim of the present work is to determine the phase diagrams for model binary lattice fluids in narrow slitlike pores with energetically nonuniform walls within a mean-field approximation. For simplicity and for transparency of interpretation of the results, we reduce the number of the parameters of the model to a minimum, by choosing the fluid–solid potential independent of the adsorbate species. The model of energetic heterogeneity is similar to that used by Röcken and Tarazona [9]. Moreover, we investigate only the model fluids with the cross interaction energy parameter low enough to ensure demixing over a wide range of temperatures and densities. The theory we apply was originally formulated by Lane [21]. Similar approaches have been subsequently applied in numerous studies of nonuniform systems [22–26]. Our principal aim is to study the formation of bridge phases and capillary condensation, as well as an interplay between these transitions and demixing inside the pore. For that reason a detailed discussion of possible layering transitions has

been omitted. Layering transitions are single-wall phenomena and their investigation by using computer simulations, as well as with the help of different theoretical approaches, has been postponed to a subsequent work.

2. Theory

Let us formulate the model first. We consider a binary fluid mixture of species '1' and '2' on a cubic lattice with vacancies (cf [21]), confined within a slitlike pore of width L_z. Each wall exerts the potential that varies in two directions, perpendicular, i, and parallel, j, to the pore wall, but is independent of the kind of adsorbate particles. Its functional form is analogous to that used by Röcken and Tarazona [9] in their studies of adsorption of a one-component fluid

$$v'(j,i) = v_0(i)[1 + a v_1(j)], \tag{1}$$

where $v_0(i)$ is the homogeneous part of the adsorbing potential and $v_1(j)$ is its periodic modulation. The integers i and j denote the consecutive lattice number along the directions perpendicular and parallel to the pore walls, respectively. The parameter a modifies the contribution due to the periodic part. The homogeneous and periodic parts are given by the following equation:

$$v_0(i) = \varepsilon_{gs}/i^3, \tag{2}$$

and

$$v_1(j) = \cos(2\pi L_x/j), \tag{3}$$

respectively. In the above L_x is the periodicity of the potential. The total adsorption energy is the sum of the contributions from the two pore walls. The first wall is a plane at $i = 0$, whereas the second wall is located at $i = L_z$. Consequently, the total adsorbing potential is $v(j,i) = v'(j,i) + v'(j, L_z - i)$ for $i = 1, 2, \ldots, L_z - 1$ and thus the number of layers available to adsorbate particles is $L_z - 1$. We are aware that the model which assumes the independence of the adsorbing potential of the kind of particles is somewhat artificial. However, the aim of the present study is to determine possible categories of the phase diagrams and for that purpose starting with a model as simple as possible seems to be the best choice.

We denote by l_x, l_y and l_z the number of the nearest neighbours in x, y and z directions, respectively. For a cubic lattice $l_x = l_y = l_z = 2$. No more than one molecule is permitted at a given lattice site and each pair of molecules in adjacent sites contributes the energy ε_{11}, ε_{22} or ε_{12} to the total potential energy, depending on the kind of interacting species.

Because of infinite repulsions (cf equation (1)), no particles can occupy the layers 0 and L_z. According to the symmetric model of the mixture, the energies $\varepsilon_{ii}(i = 1, 2)$ are identical, $\varepsilon_{11} = \varepsilon_{22} \equiv \varepsilon$. For the fluid exhibiting a partial mixing, the energy ε_{12} must be lower than ε. We use ε as the energy unit; thus the reduced temperature is defined as $T^* = kT/\varepsilon$.

The confined fluid is in contact with a bulk fluid. The total density (occupation number) of the bulk fluid is $\rho = \rho_1 + \rho_2$, where ρ_α is the density of the species α. The mole fraction of the bulk fluid is abbreviated as $x = \rho_1/\rho$.

It can be shown that in the mean-field approximation the grand potential (per layer in the y direction and per period L_x) of the system is (cf [21–26])

$$\Omega = \sum_{\alpha=1,2} \sum_{j=0}^{L_x} \sum_{i=0}^{L_z} \{v(j,i)\rho_\alpha(j,i) - \mu_\alpha \rho_\alpha(j,i)\} + kT \sum_{j=0}^{L_x} \sum_{i=0}^{L_z} \{\rho_1(j,i) \ln \rho_1(j,i) + \rho_2(j,i) \ln \rho_2(j,i) + [1 - \rho_1(j,i) - \rho_2(j,i)] \ln[1 - \rho_1(j,i)$$

$$- \rho_2(j,i)]\} - \varepsilon \sum_{\alpha=1}^{2} \sum_{j=0}^{L_x} \sum_{i=0}^{L_z} \rho_\alpha(j,i)[\rho_\alpha(j,i-1) + \rho_\alpha(j,i+1) + 2(\rho_\alpha(j-1,i) + \rho_\alpha(j+1,i))] - \varepsilon_{12} \sum_{j=0}^{L_x} \sum_{i=0}^{L_z} \rho_2(j,i)[\rho_1(j,i-1) + \rho_1(j,i+1) + 2(\rho_1(j-1,i) + \rho_1(j+1,i))] - \varepsilon_{12} \sum_{j=0}^{L_x} \sum_{i=0}^{L_z} \rho_1(j,i)[\rho_2(j,i-1) + \rho_2(j,i+1) + 2(\rho_2(j-1,i) + \rho_2(j+1,i))] \tag{4}$$

where μ_α and $\rho_\alpha(j,i)$ are the chemical potential and the local density of the species α, respectively.

The equilibrium density profile is obtained by minimizing Ω. The condition $\delta\Omega/\delta\rho_\alpha(j,i) = 0$ leads to the following set of equations:

$$\rho_1(j,i) = \frac{a_1(j,i)}{1 + a_1(j,i) + a_2(j,i)} \tag{5}$$

where

$$\ln a_1(j,i) = \frac{\mu_1}{kT} + \varepsilon[\rho_1(j,i-1) + \rho_1(j,i+1) + 2(\rho_1(j-1,i) + \rho_1(j+1,i))] + \varepsilon_{12}[\rho_2(j,i-1) + \rho_2(j,i+1) + 2(\rho_2(j-1,i) + \rho_2(j+1,i))] - \frac{v(j,i)}{kT}. \tag{6}$$

The corresponding equations for $\rho_2(j,i)$ and $a_2(j,i)$ can be easily written down by changing appropriately the species indices. The chemical potential of species 1 in a bulk system is

$$\mu_1 = kT \ln\left[\frac{\rho_1}{1-\rho}\right] - (l_x + l_y + l_z)(\varepsilon\rho_1 - \varepsilon_{12}\rho_2). \tag{7}$$

The average density of the confined fluid is computed as

$$\langle\rho\rangle = \langle\rho_1\rangle + \langle\rho_2\rangle \tag{8}$$

where

$$\langle\rho_\alpha\rangle = \frac{1}{L_x L_z} \sum_{j=0}^{L_x} \sum_{i=0}^{L_z} \rho_\alpha(j,i). \tag{9}$$

Moreover, we introduce the symbol S to abbreviate the adsorption selectivity

$$S = \langle\rho_1\rangle/\langle\rho\rangle. \tag{10}$$

To solve the density profile equations (5) one may apply a standard iteration procedure. However, quite recently Aranovich and Donohue [23, 24] proposed a new numerical algorithm to obtain multiple solutions of equation (5). They have demonstrated that their method gives the entire equilibrium curve, including points which determine wetting transitions and capillary condensation. We have adapted this method for our purposes.

The phase transition points have been determined by investigating the dependence of Ω on the chemical potentials of both species. At the transition point the excess grand potentials, $\Omega - \Omega_b$, as well as the chemical potentials of two species in coexisting phases, must be identical. In the above Ω_b is the grand potential of the bulk fluid (given by equation (2) with local densities being equal to the bulk densities everywhere). Moreover, we have examined the density profiles of different phases.

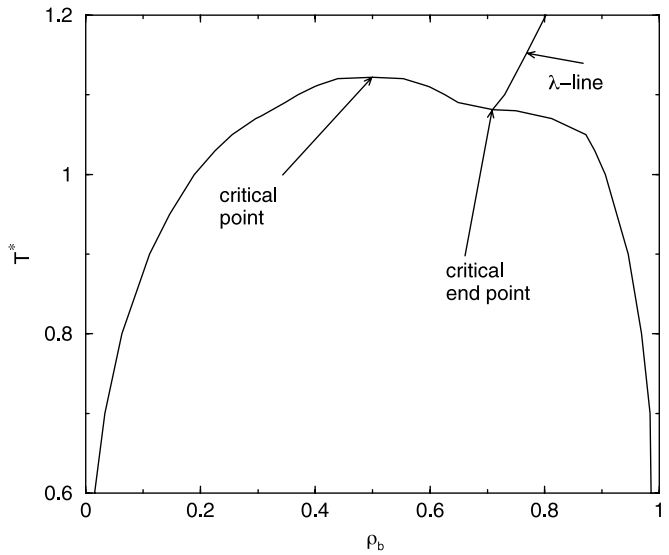

Figure 1. The phase diagram of the bulk fluid in the T^*–ρ_b plane for the model mixture with $\varepsilon_{12} = 0.5$.

3. Results and discussion

We consider a model fluid with $\varepsilon_{12} = 0.5$ and assume that the adsorption takes place from a gas phase at an equimolar composition, $x = 0.5$. To characterize the bulk system, we have evaluated the corresponding phase diagram, under the assumption that the composition of the rarefied phase is $x = 0.5$ (cf figure 1). The bulk fluid exhibits the critical point at the temperature of $T_c^* \simeq 1.12$. At the so-called critical end point temperature, $T_{CEP}^* \simeq 1.08$, the λ-line, that represents the demixing transition, departs from the liquid–vapour envelope. At the temperatures below T_{CEP}^* the condensation leads to a demixed fluid, whereas at $T_{CEP}^* < T^* < T_c^*$ the composition of the condensed phase is identical to that of the rarefied phase, $x = 0.5$.

The first calculation for confined mixtures has been performed for the pore with $L_z = 10$, $L_x = 40$, $\varepsilon_{gs} = 2$. The phase diagram for energetically uniform walls ($a = 0$) has been confronted with those evaluated for the systems of increasing energetic heterogeneity ($a = 0.2$, 0.4 and 0.6). Figure 2(a) shows the average density–temperature projections of the phase diagrams for the uniform and the heterogeneous system, characterized by $a = 0.2$. The phase diagrams have been evaluated in a usual manner, i.e. at each temperature we have plotted the values of the grand potential as a function of the chemical potential. The branches of the grand potential correspond to the consecutive branches of adsorption isotherms. A thermodynamically stable state corresponds to a minimum value of the grand potential. This point is illustrated in figure 2(b), where the arrows in the upper part indicate the equilibrium transition points; they correspond to jumps in the adsorption isotherm, displayed in the lower part of the plot. Identification of the coexisting phases has been carried out by a careful inspection of the density profiles. An identical procedure has been used for all the systems under study at all investigated temperatures.

In the case of uniform pore walls the phase diagram is composed of three branches, representing the two layering transitions and the capillary condensation. The first layering transition terminates at the tricritical point, at which the λ-line begins, while the remaining

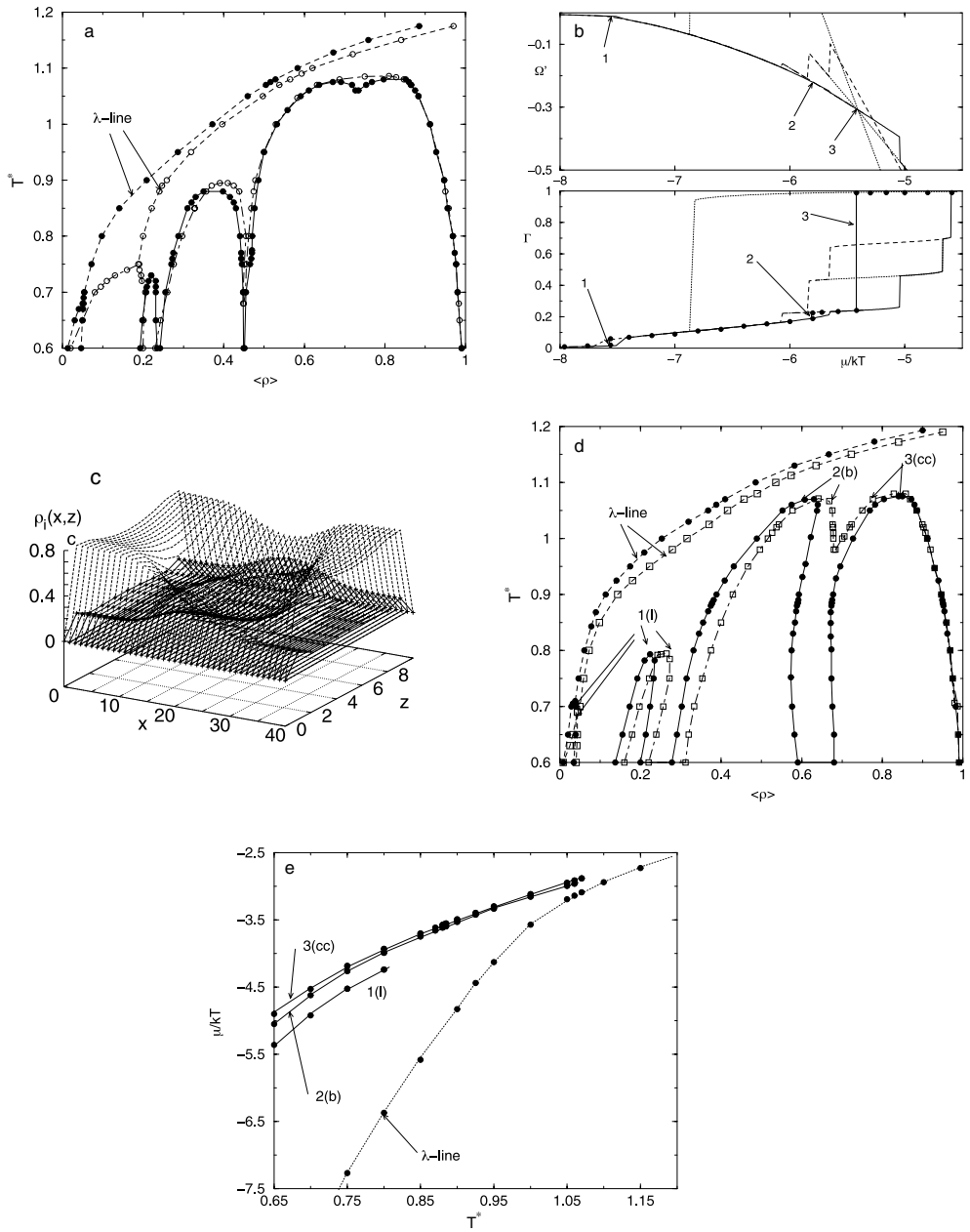

Figure 2. (a) A comparison of the phase diagrams for the pore with uniform walls—curves with open circles, and heterogeneous walls ($a = 0.2$)—curves with filled circles. (b) An example of the adsorption isotherm at $T^* = 0.6$ for the system with $a = 0.2$ (lower part) and of the grand potential $\Omega' = \Omega/AkT$ per unit surface area, A, of the pore wall (upper part). Arrows indicate the transition points. Thermodynamically stable parts of the isotherm are decorated with black circles. (c) Density profiles of two species (curves and curves decorated with points) at $T = 1.06$ at the bulk density $\rho_b = 0.1926$ just before the final capillary condensation in the system with $a = 0.2$. (d) The phase diagrams for two values of a, $a = 0.4$ (lines with open squares) and $a = 0.6$ (curves with filled circles). (e) The chemical potential—temperature projection for the system with $a = 0.6$. In all cases $L_z = 10$, $L_x = 40$ and $\varepsilon_{gs} = 2$.

transitions end at their respective critical points. This first phase diagram envelope is associated with the filling of the first layers adjacent to the pore walls. The second layering transition (counting from the side of low averaged densities) is associated with the filling of the second layer at each pore wall. The triple-point temperature separating the first and the second layering transitions is low. Performing the calculations at $T^* = 0.4$ we still observed the existence of both layering transitions. This means that the triple-point temperature is lower than 0.4. However, we did not evaluate low-temperature parts of the phase diagrams and did not study the layering transitions in detail, because these transitions are a single-wall phenomenon and the principal aim of this work has been associated with the investigation of phase transitions specific for adsorption in pores.

The high-density boundary of the second layering transition lies very close to the low-density branch of the capillary condensation. At temperatures higher than $T^* \approx 0.68$ the branches of the second layering transition and of the capillary condensation are separated; at lower temperatures they join together. Thus, the triple-point temperature separating the branches of the second layering and of the capillary condensation is approximately equal to 0.68. Note also that because the λ-line starts at the tricritical point of the first layering transition, the second layering and the capillary condensation transitions are between two demixed states. In contrast, the first layering transition occurs between a mixed (low-density) phase and a demixed layer.

The introduction of small modulation to the adsorption potential, characterized by $a = 0.2$, leads to substantial changes in the form of the phase diagram and also changes the scenario of the observed phase transformations. Inspection of the structure of the confined phases, characterized by the local densities, has revealed that the first branch (from the side of low averaged densities) is associated with the layering-type transition, taking place *only* over the most energetic parts of the surface (for the sake of brevity, we do not present the relevant local density plots here). This part of the diagram ends at the tricritical point and the tricritical point temperature is close to 0.68. Obviously, this 'partial' layering transition occurs between mixed and demixed phases. However, all remaining transitions are between two demixed states.

The second part of the diagram (at average densities in the range [0.19, 0.24]) is associated with the filling of the remaining sites, located within the *first* layer adjacent to the pore wall. The critical temperature of this transition is slightly lower than the first layering transition in a homogeneous case. The next branch, however, corresponds to the layering transition within the second layers at both pore walls and after this transition the second (and, of course, the first) layer is filled entirely. The triple-point temperature between the second layering transition and the capillary condensation is also lower than in the homogeneous pore case. Our estimation is that this temperature is approximately 0.57. Another important difference is connected with the development of the bridge phase which, however, is separated from the capillary condensation branch only at sufficiently high temperatures, above the triple point. The triple-point temperature is approximately equal to 1.05. The critical temperatures of the bridge phase and the capillary condensation are close to one another and also close to (although marginally lower than) the critical temperature of the capillary condensation in the homogeneous pore. The structure of the adsorbed fluid after the bridge phase formation, but before the final capillary condensation, is shown in figure 2(c). Compared with a homogeneous pore, the λ-line is moved toward lower average densities.

Further increase of the surface potential modulation, to $a = 0.4$ and 0.6 (cf figure 2(d)), results in deepening of the changes observed for a weakly heterogeneous pore of $a = 0.2$. Namely, the λ-line again shifts in the direction of lower average densities, the triple-point temperature between the bridge and capillary condensation decreases and for $a = 0.6$ it falls well below the lowest temperature considered (or does not exist at all; at $T = 0.4$ we have

still observed the existence of two, well separated braches). Heterogeneity does not seem to have a pronounced effect on the critical temperatures of the bridge phase and the capillary condensation. However, there is one important difference compared with the case of $a = 0.2$. For both values of $a = 0.4$ and 0.6 the first branch of the phase diagram is associated with the layering transition within the first layer over the most energetic parts of the surface. The second branch, however, is for the layering transition, taking place within the *second* layer, but still over the most energetic adsorbing sites, whereas in the case of $a = 0.2$ the second branch corresponds to the filling of the low-energy sites within the first layer. This quantitative difference in the phase behaviour explains why the critical temperatures of the second branch of the phase diagram for $a = 0.2$ and for $a = 0.4$ and 0.6 behave in a non-monotonic manner. We stress again: after that transition the low-energy sites, located within the second and within the first layers, remain empty. They are filled during the next phase transition. The triple-point temperatures between the first and the second branches, as well as between the second branch and the capillary condensation envelope, if they exist, are quite low. When the heterogeneity parameter a increases, the two 'partial'-layering transitions ('partial' because they do not obey the entire layers, but only the sites over the most energetic surface centres) are shifted toward lower average densities.

As we have already noted, the λ-line is also shifted in the direction of low average densities as a increases. It starts at the tricritical point of the first 'partial' layering transition. For $a = 0.4$ the tricritical point occurs at temperature close to 0.69 and for $a = 0.6$ at temperature approximately equal to $\approx$0.71. Therefore, we conclude (cf also figure 2(a)) that the heterogeneity slightly increases the tricritical point temperature.

The main part of the phase diagram is connected with a filling of the entire pore. It means that this part of the diagram is also associated with the filling of the first- and of the second-layer sites, located over weakly attractive sites on the surface. Already for $a = 0.4$ we observe the formation of a bridge phase at sufficiently high temperatures, which results in splitting the coexistence envelope into two parts. These two parts meet at the triple point, so that at still lower temperatures the capillary condensation becomes a one-step process. Above the triple-point temperature (equal approximately to 0.98 for $a = 0.4$), the adsorbed phase fills the bridges over the most energetic parts of the surface. However, all sites over weakly adsorbing parts remain only partially filled (within the first layer) or nearly completely empty (within the consecutive layers). They are finally filled during the second step of the capillary condensation.

The increase of a leads to rather abrupt lowering of the triple-point temperatures. Thus, for $a = 0.6$ we observe a complete separation of the two steps of the condensation process over the entire range of the temperatures used. This separation has been also observed at temperature as low as 0.4. Therefore, the triple point between the bridge phase formation and the capillary condensation, if exists at all, would appear at a quite low temperature.

Figure 2(e) brings an example of the chemical potential–temperature projection of the phase diagram for $a = 0.6$, which also clearly demonstrates the separation of different phases.

The effect of the period length, L_x, on the phase behaviour is illustrated in figure 3, which shows the density–temperature phase diagrams, obtained for $\varepsilon_{gs} = 2, a = 0.8$ and $L_x = 22, 40$ and 80. The scenario of the phase transformations is the same as for $a = 0.6$ in figure 2(c). We observe that the λ-line is only weakly affected by the value of L_x and slightly moves toward higher average densities as L_x decreases. Again, the λ-line begins at the tricritical point, ending the first, partial layering. In particular, for the largest value of the period, $L_x = 80$, the tricritical temperature is about 0.72. For lower values of L_x the tricritical point is shifted toward lower temperatures: for $L_x = 40$ it appears at the temperature approximately equal to 0.715, whereas for $L_x = 22$ at $T^* \approx 0.64$.

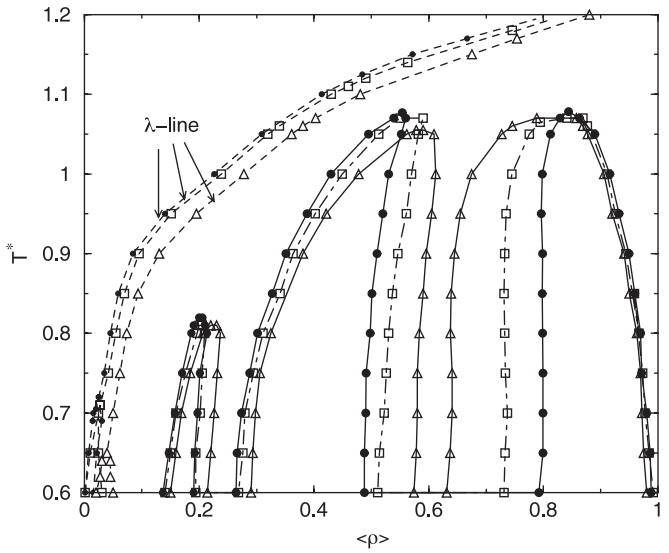

Figure 3. The phase diagrams for $L_z = 10$, $\varepsilon_{gs} = 2$, $a = 0.8$ and $L_x = 22$ (curves with triangles), $L_x = 40$ (curves with squares) and $L_x = 80$ (curves with circles).

The second 'partial' layering transition, which similarly as previously is the transition within the second layer sites over the highly energetic parts of the surface, is slightly affected by the change of the period length and shifts in the direction of lower average densities with increasing L_x. After that transition weakly energetic sites within the first layer remain still incompletely filled. On the other hand, the locations of the bridge phase and of the capillary condensation parts depend considerably more strongly on L_x. The increase of L_x results in a more pronounced separation of those two branches of the phase diagram. Decreasing the temperature to $T^* = 0.4$ we still have not observed any triple points between the layering, bridge phase and capillary condensation branches for the chosen values of energetic parameters. Those points, if they exist, may appear at quite low temperatures.

Four panels of figure 4 present local density surfaces for the system $\varepsilon_{gs} = 2$, $a = 0.8$, $L_x = 40$ and $L_z = 10$, obtained at the temperature of $T^* = 0.7$ and at different densities. Figure 4(a) illustrates an early stage of continuous demixing ($\langle\rho\rangle = 0.094$). Only the strongly adsorbing sites of the layers adjacent to the pore walls are partially filled. The density profiles of components 1 and 2 at $\langle\rho\rangle = 0.574$, i.e. in the region between the bridge phase and the capillary condensation coexistence, are given in figures 4(b) and (c), respectively. The bridge phase is mainly composed of one component, while the second component accumulates mostly at the boundary region of the bridge phase, as well as in the surface region over weakly adsorbing sites. Finally, figure 4(d) shows the density profiles of both species, obtained at the state point after the capillary condensation, $\langle\rho\rangle = 0.992$. In this case the demixing is nearly completed. Of course, the density profile for the dense phase filling the entire pore is almost insensitive to the lateral variation of the surface field.

The effect of the pore width on the phase behaviour is illustrated in figure 5, which shows the results evaluated for two different values of $L_z = 7$ and 10 and the fixed values of all remaining parameters ($\varepsilon_{gs} = 2$, $a = 0.4$ and $L_x = 40$). The results for $L_z = 10$ have already been presented (figure 2(d)) and discussed. The lowering of the pore width to $L_z = 7$ considerably changes the conditions at which the bridge phase and the capillary

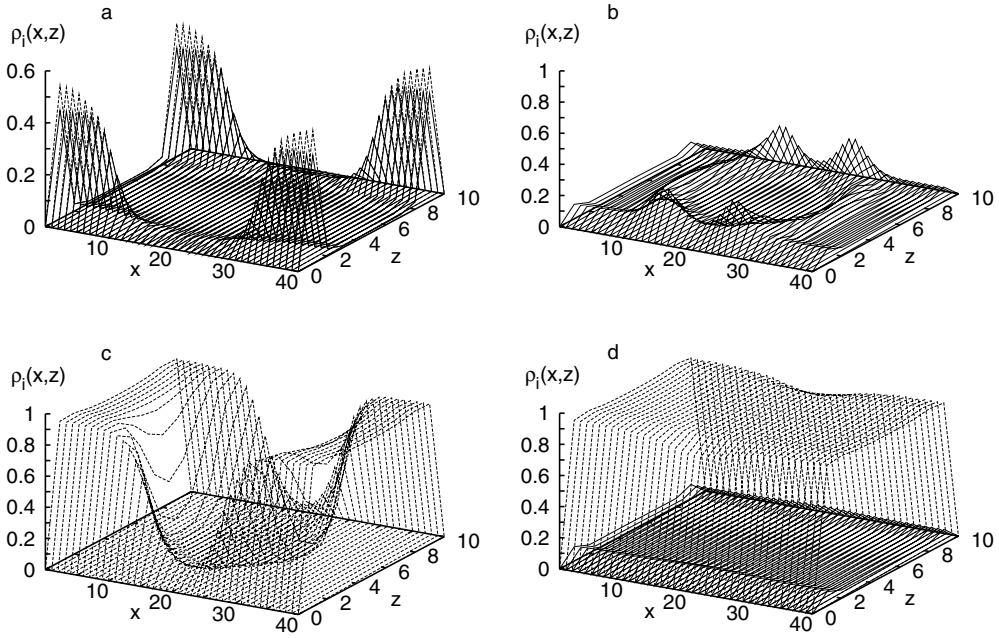

Figure 4. Examples of the local density surfaces for the system with $L_z = 10$, $\varepsilon_{gs} = 2$, $a = 0.6$ and $L_x = 40$ at three state points. (a) After the λ-line, $\langle\rho\rangle = 0.094$. (b), (c) Density surfaces for both components after the bridge phase formation, $\langle\rho\rangle = 0.574$. (d) After the capillary condensation, $\langle\rho\rangle = 0.992$. Solid and dashed lines are for different components.

condensation take place. The low-density boundary for the bridge phase coexistence moves toward lower average densities and the entire bridge phase envelope decouples from the capillary condensation coexistence. Moreover, the second 'partial' layering transition (within the second layer), present for $L_z = 10$, vanishes for $L_z = 7$. Therefore, the sequence of the phase transformations for $L_z = 7$ is the following. At low temperatures we first observe the first partial layering, which takes place over the most energetic centres within the first layer. This transition ends at the tricritical temperature, which is very close to 0.7 and thus it is slightly higher that for $L_z = 10$. Compared with the pore of $L_z = 10$, the λ-line moves in the direction of higher average densities. The second transition in the pore of $L_z = 7$ is associated with the formation of bridges 'connecting' the highly energetic sites at both pore walls. After that transition, the sites located over weakly attracting surface centres remain only partially filled. Final filling of those sites occurs during the second stage of the capillary condensation. For $L_z = 7$ the triple-point temperature between bridge phase formation and the capillary condensation is strongly reduced (or the triple point does not exist at all; two branches have been also observed at $T^* = 0.4$).

Figure 6 illustrates some interesting changes in the form of the phase diagram due to changes in the homogeneous part of the adsorption energy. The results presented here have been obtained for the systems with $\varepsilon_{gs} = 1$, $a = 0.6$, $L_x = 40$ and $L_z = 7$, i.e. the homogeneous part of the adsorption potential is twice as weak as in the cases considered so far. Even in the case of weaker adsorbing walls, as compared to the results shown previously, the filling of the pore occurs in two steps. The first step corresponds to the bridge phase formation. The second step is the capillary condensation. Similarly as previously we also observe the existence of the partial layering transition within the first layer. This layering transition ends at the tricritical temperature, which is close to 0.66.

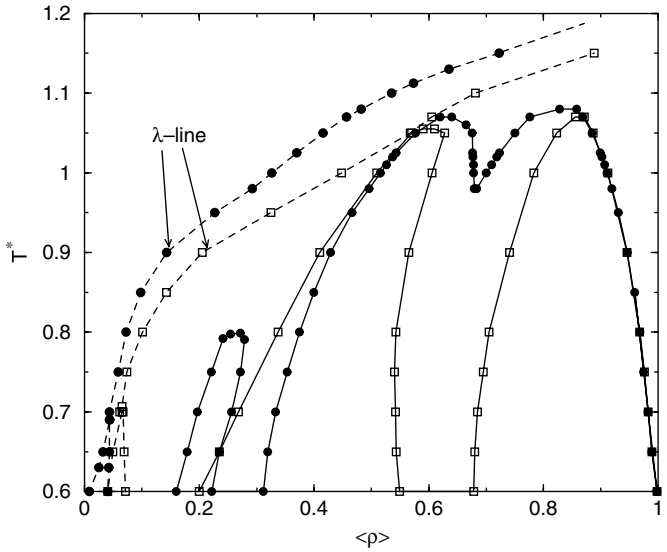

Figure 5. The phase diagrams for $L_x = 40$, $\varepsilon_{gs} = 2$, $a = 0.4$ and $L_z = 10$ (curves with circles) and $L_x = 7$ (curves with squares).

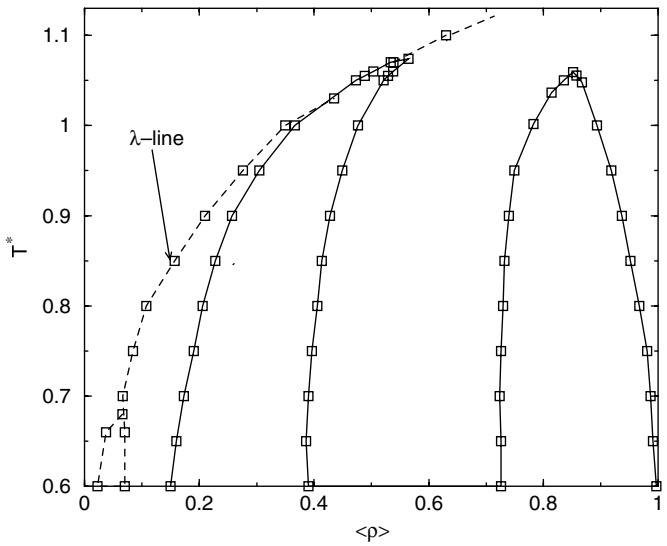

Figure 6. The phase diagrams for $L_x = 40$, $\varepsilon_{gs} = 1$, $a = 0.6$ and $L_x = 7$.

To illustrate the scenario of the phase transformations at low temperatures we have included the plots of the density profiles at some selected state points at $T^* = 0.6$. Figures 7(a) and (b) show respectively the profiles of both components just before and just after the first, partial layering transition, $\rho_b = 0.003\,28$. The profiles in figure 7(a) flow together; the adsorbed phase is mixed. In figure 7(b) the first layer over the most energetic surface centres is filled. All remaining sites inside the pore remain nearly empty. The adsorbed phase is demixed. Figure 7(c) gives an insight into the structure of the adsorbed fluid just after the bridge phase

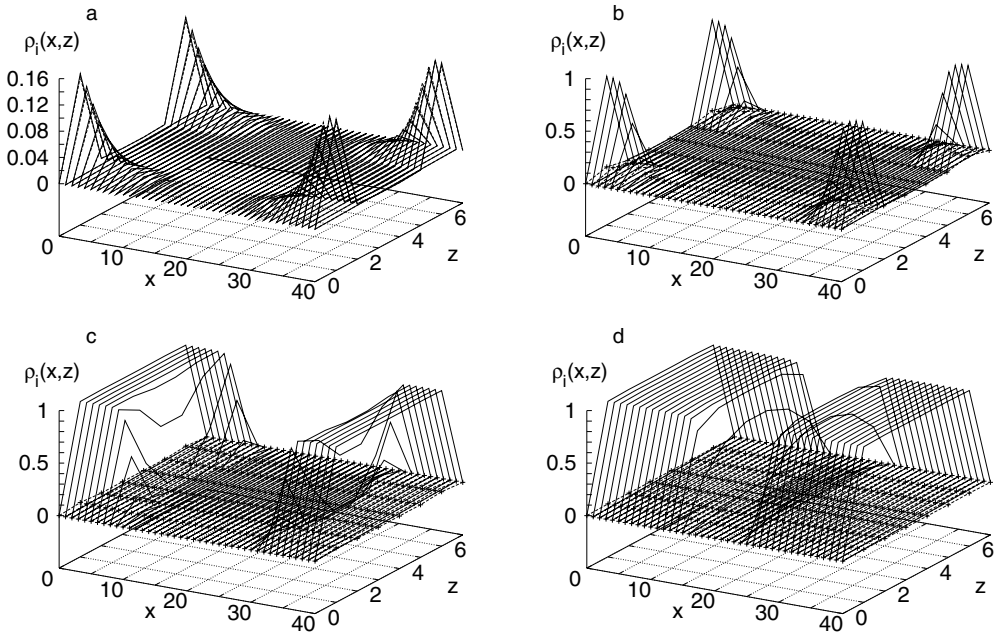

Figure 7. Examples of the local densities for the system shown in figure 6 at $T^* = 0.6$. (a) and (b) show the structure just before and just after the first partial layering transition, $\rho_b = 0.003\,28$, (c) after the bridge phase formation, $\rho_b = 0.0081$, and (d) just before the capillary condensation, $\rho_b = 0.015\,76$. The profile of one component in (b), (c) and (d) is shown by a line decorated with points. In (a) the profiles of both components flow together.

formation, $\rho_b = 0.0081$. All the sites over weakly adsorbing surface centres are nearly empty. Obviously, the adsorbed phase is demixed. Finally, figure 7(d) shows the situation just before the final capillary condensation, $\rho_b = 0.015\,76$. The weakly adsorbing sites still remain nearly empty. Capillary condensation causes these sites to be filled. After the capillary condensation the structure of the adsorbed fluid is almost independent of the lateral changes of the adsorption potential (cf figure 4(d)).

An interesting observation concerns the behaviour of the λ-line. Namely, this line crosses the bridge part of the phase diagram. Therefore, two, lower and upper, critical end points appear. In consequence, the character of the bridge phase formation changes with temperature. At temperatures below the lower critical end point the transition is between two demixed phases. Over the temperature range between the two critical end points the transition leads from a mixed to demixed phase. Finally, above the upper critical end point (but, of course, below the critical point) the transition again takes place between two demixed phases.

To conclude, we have investigated the phase behaviour of the lattice binary symmetric mixture confined to energetically heterogeneous slitlike pores by using the mean-field approach. The bulk model is characterized by weak interaction between unlike particles that results in an interplay between the first-order and continuous demixing transitions. In confined systems condensation occurs in several steps. It consists of layering transitions, the bridge phase formation and, finally, the filling of the entire pore if the adsorbing field is strong enough. Energetic heterogeneity drives the layering branches narrower because the condensed phases occur only over the strongly adsorbing parts of the pore walls. The λ-line of the demixing transition shifts to lower average densities as compared to the pore with homogeneous walls.

It starts at the coexistence curve of the first layering transition. In the systems studied it always begins at the tricritical point. However, it is possible that the beginning of this line may be located at the critical end point. The position of that line is less sensitive to energetic heterogeneity compared to the first-order transitions. For L_z large enough (in our case for $L_z = 10$) a step-wise condensation occurs between demixed phases. For narrower pores, however, the λ-line may cross the boundaries of the bridge phase and multiple critical end points appear. In such cases, the bridge phase formation occurs via re-entrant transition in the following way. At low temperatures the transition takes place between demixed phases, at intermediate temperature it involves mixed and demixed phases and finally it becomes a transition between two demixed phases again. Our computations have been performed for a specific model. One should take into account that changing the model of the mixture, or the model of the surface heterogeneity, may result in different kinds of phase behaviour of confined mixtures.

Acknowledgments

This work was supported by CONACyT (grant 37323-E) and by UNAM (grant IN113101).

References

[1] Patrykiejew A and Borowko M 2001 *Computational Methods in Surface and Colloid Science* ed M Borowko (New York: Dekker) ch 5
[2] Rudzinski W and Everett D H 1992 *Adsorption of Gases on Heterogeneous Surfaces* (New York: Academic)
[3] Sundarem M, Chalmers S A, Hopkins P F and Gossard A C 1991 *Science* **254** 1326
[4] Rauscher H, Jung T A, Lin J-L, Kirakosian A, Himpsel F J, Rohr U and Küllen K 1999 *Chem. Phys. Lett.* **303** 363
[5] Knight J B, Vishwanath A, Brody J P and Austin R H 1998 *Phys. Rev. Lett.* **80** 3863
[6] Grunze M 1999 *Science* **283** 41
[7] Netz R R and Andelman D 1997 *Phys. Rev.* E **55** 687
[8] Reszko-Zygmunt J, Rżysko W, Sokołowski S, Sokołowska Z and Pizio O 2001 *Mol. Phys.* **99** 1589
[9] Röcken P and Tarazona P 1996 *J. Chem. Phys.* **105** 2034
[10] Röcken P, Somoza A, Tarazona P and Findenegg G H 1998 *J. Chem. Phys.* **108** 8689
[11] Millan B, Pizio O, Patrykiejew A and Sokołowski S 2001 *J. Phys.: Condens. Matter* **13** 1361
[12] Reszko-Zygmunt J, Pizio O, Rżysko W and Sokołowski S 2001 *J. Colloid Interface Sci.* **241** 169
[13] Diestler D J and Schoen M 2000 *Phys. Rev.* E **52** 5515
[14] Bock H, Diestler D J and Schoen M 2001 *Phys. Rev.* E **64** 046124
[15] Rowlinson J S and Swinton F L 1982 *Liquids and Liquid Mixtures* (London: Butterworth)
[16] van Konynenburg P H and Scott R L 1980 *Phil. Trans. R. Soc.* A **298** 495
[17] Vidales A, Benavides A L and Gil-Villegas A 2001 *Mol. Phys.* **99** 703
[18] Wang J-L, Wu G-W and Sadus R J 2000 *Mol. Phys.* **98** 715
[19] Kahl G, Schöll-Paschinger E and Lang A 2001 *Mon. Chem.* **132** 1413
[20] Wilding N B, Schmid F and Nielaba P 1998 *Phys. Rev.* E **58** 2201
[21] Lane L E 1968 *Aust. J. Chem.* **21** 827
[22] De Oliviera M J and Griffiths R B 1978 *Surface Sci.* **71** 687
[23] Aranovich G L and Donohue M D 1998 *J. Colloid Interface Sci.* **200** 273
[24] Aranovich G L and Donohue M D 1999 *Phys. Rev.* E **60** 5552
[25] Pilorz K and Sokołowski S 1984 *Z. Phys. Chem.* **265** 929
[26] Zagórski R and Sokołowski S 2001 *J. Colloid Interface Sci.* **240** 219